

## Temperature patterns on a hollow cylindrical catalytic pellet

J. Annamalai, M. A. Liauw,<sup>a)</sup> and D. Luss<sup>b)</sup>

*Department of Chemical Engineering, University of Houston, Houston, Texas 77204-4792*

(Received 26 August 1998; accepted for publication 23 November 1998)

The atmospheric oxidation of a mixture containing 6 vol % carbon monoxide was carried out on a hollow cylindrical catalytic pellet. The catalyst was held in a conical reactor which enabled simultaneous measurement of the temperature patterns on the top and side of the pellet by an IR imager. Upon a decrease in the reactor temperature the fully ignited, high temperature state of the pellet is transformed to a nonuniform one with temperature fronts separating high and low temperature regions. The transition and the resulting states are rather intricate and are strongly influenced by the nonuniformity of the catalyst and the transport to and from it, as well as the global coupling, which stabilizes temperature fronts and patterns, which would not exist in its absence. Intricate pulse splitting and extinction were observed both on the top and the side of the pellet. Highly irregular motions and conversions were obtained following a decrease in the reactor temperature. © 1999 American Institute of Physics. [S1054-1500(99)00901-5]

**When an exothermic, atmospheric reaction is carried out on a catalytic surface, its surface temperature exceeds that of the ambient fluid. The length scale of the surface temperature, which is the autocatalytic variable in the system, is for most high-pressure, exothermic reactions much longer than that of all the other dynamic surface variables, such as surface activity or concentration. Thus, it was assumed for a long time that the catalyst surface temperature is uniform. However, experiments revealed that a rich variety of temperature patterns exist. These patterns may have a significant impact on the performance of catalytic pellets used in very many important industrial processes. Experiments using a thin ring revealed that the temperature patterns are stabilized by global coupling and are affected by the nonuniformity of the catalyst activity. This study is part of a systematic effort to gain an understanding of patterns on more complex geometries, as industrial catalysts and catalyst bed are three-dimensional bodies. Specifically, we measure by an IR imager and a special conical mirror, the top and side temperature patterns on a thin hollow cylindrical pellet, which catalyzes the oxidation of carbon monoxide. While some of the spatiotemporal temperature patterns are similar to those observed on a thin ring, some are more intricate. A reduction in the reactor temperature tends to destabilize the temperature fronts. The global coupling counteracts changes in the overall reaction rate, and the catalyst nonuniformity affects the direction and velocity of the temperature fronts.**

### I. INTRODUCTION

Spatiotemporal pattern formation is a ubiquitous phenomenon. Moving fronts, spiral waves, standing waves are

some of the many patterns that have been observed in systems as different as slime molds, electric discharge, brain activity and others.<sup>1</sup>

Insights stemming from extensive theoretical studies and numerical simulations of nonlinear dynamic systems have been accompanied by fascinating experimental results. While the Belousov-Zhabotinskii reaction may be considered the workhorse of homogeneous reaction-diffusion systems, the study of the dynamics of heterogeneous catalytic reactions has become increasingly important. Pioneering studies by Ertl and co-workers on pattern formation under UHV conditions have drawn attention to pattern formation in these systems.<sup>2,3</sup> Our research, as that by several other groups, has focused on catalysis at atmospheric pressure with the goal of understanding and being able to predict the features and impact of temperature patterns on industrial catalytic processes.

Early research was on one-dimensional model systems with nonperiodic boundary conditions. Following work by Busch<sup>4</sup> and Barelko *et al.*,<sup>5</sup> electrically heated ribbons have been studied by Lobban *et al.*,<sup>6</sup> Lobban and Luss,<sup>7</sup> Sheintuch and Schmidt,<sup>8</sup> Cordonier and Schmidt,<sup>9</sup> Cordonier *et al.*,<sup>10</sup> Philippou *et al.*,<sup>11</sup> and Philippou and Luss.<sup>12</sup> The use of infrared thermography to monitor spatiotemporal surface temperatures, introduced by Schmitz's group,<sup>13,14</sup> significantly enhanced the study of these thermal patterns.

Even though interesting patterns like stationary and moving temperature fronts were observed, the heat losses at the ends of the ribbons eventually turned out to have an overwhelming impact on pattern selection. The studies were hence redirected to one-dimensional model systems with periodic boundary conditions, catalytically active thin rings. Close inspection of stationary<sup>15</sup> and moving<sup>16-18</sup> hot spots on such rings revealed two crucial phenomena frequently encountered in heterogeneous catalytic systems. First, the hot spots are stabilized by a global coupling mechanism. Any attempt of the hot spot to, say, grow wider, would decrease the concentration of the deficient compound in the gas phase and hence arrest the front motion. This has been studied theoretically by Middy *et al.*<sup>19</sup> Second, angular periodic

<sup>a)</sup>Present address: Lehrstuhl für Technische Chemie I, Friedrich-Alexander Universität Erlangen-Nürnberg, Egerlandstrasse 3, D-91058 Erlangen, Germany.

<sup>b)</sup>Author to whom correspondence should be addressed.

variation of the speed of a hot spot traveling around a ring indicates an intrinsic nonuniformity of system properties. The effect of such inhomogeneities has, e.g., been described in simulation studies by Liauw *et al.*,<sup>20</sup> Shvartsman *et al.*,<sup>21</sup> and Sheintuch.<sup>22</sup>

Useful as the ring geometry may prove to study spatiotemporal pattern formation, most systems of practical interest display more complicated geometries. One step towards these systems consists in studying patterns on two-dimensional model systems with nonperiodic boundary conditions, catalytically active disks or wafers.<sup>23–25</sup> Complex behavior found by Lane *et al.*<sup>26</sup> was again convincingly explained with nonuniformity and global coupling.

This paper takes the quest for real-life geometries yet another step further. The system under scrutiny is a hollow, thin cylindrical catalytic pellet, which may be looked upon as a two-dimensional model system with a periodic boundary condition. Combining the infrared thermography with a conical mirror allows for monitoring the temperature distribution on both the top and outside of the cylinder as a function of time. Note that the inevitable nonuniformity of catalyst properties is accompanied by intrinsic changes of gas phase composition and flow along the axis, and again by a global coupling via the gas phase concentrations. It should be noted that the propagation of waves over two and three dimensional structures is commonly encountered in biological heart tissue (see Chaos, March 1998 Focus Issue on this subject) or electrochemical systems.<sup>27–29</sup>

## II. EXPERIMENTAL SYSTEM AND PROCEDURE

An IR imager was used to measure temperature patterns during the atmospheric oxidation of carbon monoxide on a hollow, cylindrical (28 mm i.d., 38 mm o.d., and 16 mm long) catalytic pellet of 0.9 wt. % Pd on alumina. It was made by pressing (1.5 tons/cm<sup>2</sup>), in a die, a palladium on alumina powder (1% Pd; Aldrich) thoroughly mixed with a liquid alumina hardener (A17401; Zircar). The pellet was placed in a conically shaped stainless steel reactor (118 mm top diameter, 38 mm bottom diameter, conical section 40 mm high, total height 89 mm, total volume of 492 cm<sup>3</sup>) on the tips of three vertically placed, sharp-tipped pins. The reactor lid was a quartz window. The reactor inside walls were polished and gold coated to provide a nonreactive, IR-reflective surface. The conical surface was inclined by 45° with respect to the horizontal plane so that the infrared radiation from the catalyst side was reflected upwards and normal to the quartz plate. The IR radiation from the top and side of the catalyst pellet was measured by an Amber Radiance PM infrared camera with a 256×256 indium-antimonide detector array. A mirror was used to enable the camera to view the catalyst at a distance from the oven (see Fig. 1) with a spatial resolution of 0.4 mm<sup>2</sup>. The 256×256 image was recorded on a PC (generally, at the rate of 1 image every minute) using Imagedesk II (software; Amber). Special temperature calibration was done to account for the infrared absorption and emission of the quartz reactor lid.

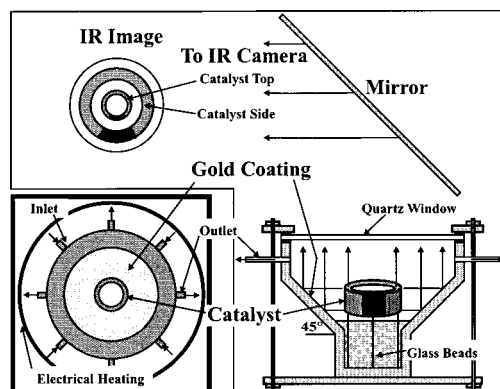


FIG. 1. Bottom of figure are schematic top (left) and side (right) views of the reactor and catalyst pellet. Top of figure shows the mirror and a typical IR image. The black color (on part of the catalyst) indicates that the temperature in that area differs from that around it.

The reactor was placed inside an insulated oven and its wall temperature controlled with a PID controller (Omega CN2041).

The incoming gases were fed through four angularly symmetric inlet ports (4.7 mm i.d.) located 13 mm upwards from the reactor bottom, which was filled with glass beads (3 mm diam) to distribute the feed. The effluent exited through four similar ports at the reactor top (4.7 mm i.d., shifted by 45° with respect to the inlet ports and 64 mm upwards). The feed gases were certified grade mixture of 30 vol % carbon monoxide and 70 vol % nitrogen (Aeriform), purified grade nitrogen (99.998% pure) and extra dry grade oxygen (purity 99.6%). The carbon monoxide was passed through a carbonyl trap of a molecular sieve adsorbent (5A zeolite; Linde) kept at 240 °C. The feed gases were mixed in a bed of glass beads, purified, and dried by activated charcoal purifiers (Linde) before entering the reactor. The gas flow rates were controlled by thermal mass flow controllers (FC-280, FC-261, and FC-260; Tylan; accuracy  $\pm 1\%$ ). The effluent carbon monoxide concentration was continuously monitored with an infrared analyzer (AR-411; Anarad). No reaction was detected in the empty reactor (without catalyst) when heated up to 200 °C.

## III. EXPERIMENTAL RESULTS

Mixtures containing 6 vol % carbon monoxide, 70 vol % oxygen and 24 vol % nitrogen were used as the feed to the reactor in which the carbon monoxide was oxidized on the catalytic pellet. Unless otherwise specified, the feed flow rate was 800 cm<sup>3</sup>/min (at room temperature), so that the space time (reactor volume divided by reactant volumetric flow rate at room temperature) was 35 s. The catalyst was bistable and the low conversion, low temperature, extinguished state ignited at about 170 °C. Upon cooling the fully ignited, high-temperature state shifted at about 85 °C to a nonuniform state, in which temperature fronts separated regions with high and low temperatures. This nonuniform state persisted even with no external heating.

Typical states observed as the reactor temperature was decreased are shown in Fig. 2. Fig. 2(i) describes four instantaneous observations of the temperature at the top of the

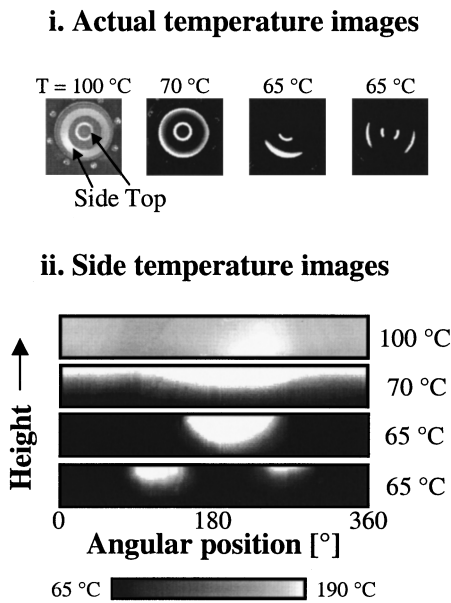


FIG. 2. The transition from a fully ignited to a nonuniform state upon a decrease in reactor temperature for a feed flow rate of  $800 \text{ cm}^3/\text{min}$ . (i) Infrared images of the pellet top (inner ring) and side (outer ring) at different reactor wall temperatures. (ii) Dependence of the instantaneous catalyst surface temperature on the axial and angular position.

pellet (inner circle) and on its side (external circle). For the sake of clarity, bar views [Fig. 2(ii)] of the instantaneous temperature patterns on the side of the pellet are presented below the four actual images. The temperature at the top of the pellet is very close to that on its upper part. When the reactor wall temperature was  $100^\circ\text{C}$  the pellet was fully ignited. At about  $85^\circ\text{C}$  a cold, stationary region formed at the bottom of the pellet. It propagated upwards upon further cooling of the reactor. At  $70^\circ\text{C}$  the lower half of the pellet was extinguished, while a small hot region existed at the top. The reactor carbon monoxide concentration and the maximum pellet temperature increased as the reactor was cooled. When the reactor was kept at  $65^\circ\text{C}$  a hot region formed, which was smaller but deeper than that at  $70^\circ\text{C}$  [see Fig. 2(ii)]. This hot region then expanded and became shallower. It eventually split into two distinct hot regions [see the two states at  $65^\circ\text{C}$  in Fig. 2(ii)]. The two hot regions moved and eventually one extinguished and the other expanded back to the size of original single hot zone. This repeated pulse splitting and extinction of one of the two pulses is apparent from the angular position-time dependence of the temperature on the top of the pellet [Fig. 3(i)]. The five maps of the instantaneous temperature dependence on height and angular position [Fig. 3(ii)] show the change in depth of the hot zone and its periodic (period of about 2 h) splitting and subsequent extinction of one of the two hot regions. The corresponding reactor CO outlet concentration [Fig. 3(iii)] decreased as the hot zone expanded. A marked increase in CO concentration was noticed as the hot region split to two small ones. When one of the two hot regions extinguished, the decreased reaction rate caused another small increase in the CO effluent concentration. The concentration of the CO decreased monotonically as the single zone expanded.

A periodic generation and extinction of a second hot

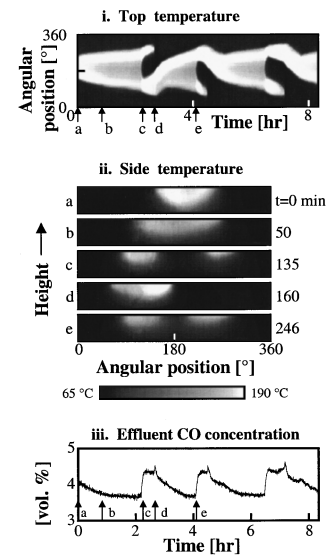


FIG. 3. Temporal temperature and reactivity of the catalytic pellet in a reactor kept at  $65^\circ\text{C}$ . (i) Surface temperature of the catalyst top as a function of time and angular position. (ii) Instantaneous catalyst side temperature as a function of axial and angular position. The times correspond to those marked by arrows (a)–(e) in (i). (iii) Corresponding effluent CO concentration.

zone (backfiring) on the top of the pellet occurred also at a reactor temperature of  $55^\circ\text{C}$  [Fig. 4(i)]. In this case, the two hot zones existed for a longer fraction of the period than that at  $65^\circ\text{C}$  [Fig. 3(i)]. The instantaneous temperature pro-

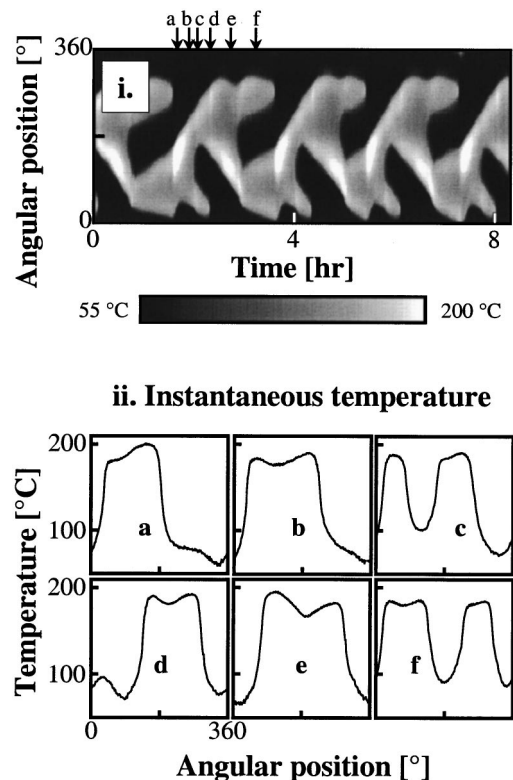


FIG. 4. The temperature at the top of the pellet in a reactor at  $55^\circ\text{C}$ . (i) Temperature as a function of time and angular position. (ii) Instantaneous temperature profiles at times corresponding to arrows (a)–(f) in (i).

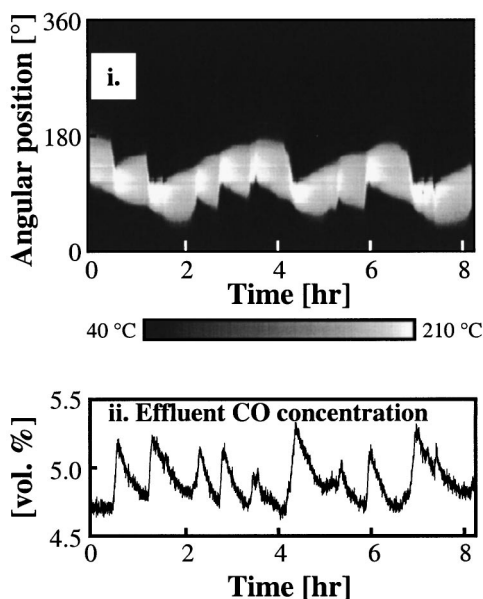


FIG. 5. Back and forth motion of a hot zone when the reactor is at 40 °C. (i) Catalyst top surface temperature as a function of time and angular position. (ii) Corresponding effluent CO concentration profile.

files at six different times [Fig. 4(ii)] clearly illustrate the periodic wave splitting (backfiring) and subsequent extinction of one of the two hot regions.

When the reactor was further cooled to 40 °C a single narrow hot zone formed at the top of the catalyst, which moved in an irregular fashion back and forth [Fig. 5(i)]. The corresponding effluent reactant concentration changed in an irregular way. Due to the rather low frequency of the motion (oscillation period exceeding half an hour) it was not practical to collect data over the long period needed to characterize this irregular time series.

Increasing the flow rate shifted the transition between the ignited and the nonuniform state to lower reactor temperatures, but did not change the qualitative features from those observed at a flow rate of 800 cm<sup>3</sup>/min. For example, at a flow rate of 1600 cm<sup>3</sup>/min, the pellet remained at an ignited state until the reactor temperature was about 40 °C. The spatiotemporal temperature pattern on top of the pellet changed after about 7 h for a reactor wall temperature of 33 °C [Fig. 6(i)]. Similar slow evolution and temporal changes in the temperature pattern features were observed in other experiments. The corresponding effluent CO concentration [Fig. 6(ii)] was rather irregular, as it was in Fig. 5(ii) for a similar reactor temperature.

The behavior at a flow rate of 400 cm<sup>3</sup>/min (Fig. 7) was similar to that at higher flow rates but no splitting of the hot zone was observed. A stationary hot pulse was obtained at high temperatures. Cooling decreased its width, increased its maximal temperature and caused a back-and-forth motion of the temperature fronts. This motion became more erratic upon reduction in the reactor temperature.

The intrinsic activity of catalytic pellets is usually non-uniform. To check this effect experiments were conducted with the pellet turned upside down. This rotation of the pellet changed the type of temperature patterns generated. How-

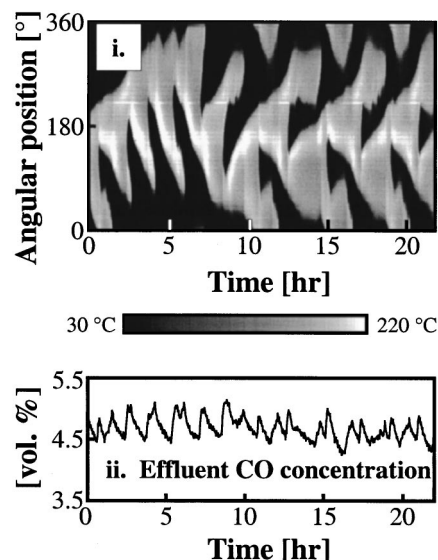


FIG. 6. Irregular behavior observed when the reactor temperature is 33 °C and the feed flow rate is 1600 cm<sup>3</sup>/min. (i) Top of pellet temperature as a function of time and angular position. (ii) The corresponding effluent CO concentration profile.

ever, when the original pellet position was restored, the original type patterns were obtained. Typical temperature patterns of the upside down turned pellet are shown in Fig. 8. At 105 °C, the pellet was fully ignited. Additional cooling generated an extinguished zone which extended from the bottom to the top of the pellet. At 90 °C two connected hot zones existed, one at the bottom and one at the top. In contrast, when the pellet was not turned upside down, the whole bottom of the pellet cooled while the top remained ignited as the temperature was decreased [Fig. 2(ii)]. At 65 °C two hot zones existed, one at the bottom of the reactor, and one that extended from the bottom to the top. At 55 °C two hot zones existed, one at the top and one at the bottom of the pellet.

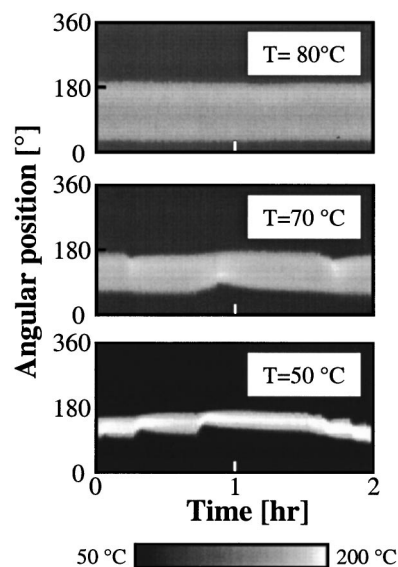


FIG. 7. Influence of changes in the reactor temperature on the hot zone for a feed flow rate of 400 cm<sup>3</sup>/min.

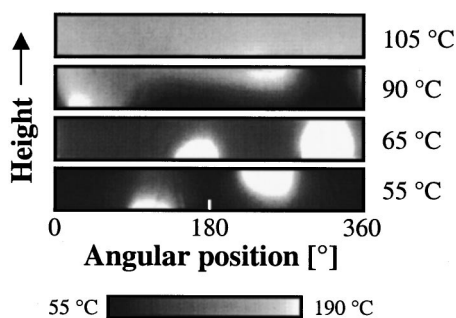


FIG. 8. Dependence of the pellet side temperature on the reactor temperature for the upside down turned pellet.

The cross sections of the two zones were smaller than those formed at 90 °C, but extended further from the top and bottom and had a higher maximal temperature.

A periodic formation of two hot zones and subsequent extinction of one of those occurred at 39 °C and a flow rate of 1600 cm<sup>3</sup>/min [Fig. 9(i)]. Initially, at  $t=0$  min a large hot zone existed, which extended from the bottom to the top of the pellet. At  $t=15$  min, the hot zone split so that two distinct hot zones existed at the bottom of the pellet. The two zones were connected at the upper part of the pellet and only one zone existed at the top of the pellet. The instantaneous temperature pattern on the pellet side at  $t=15$  min resembles that obtained during pulse splitting on the top of the pellet (see Fig. 4) At  $t=50$  min two distinct hot zones existed, which extended from the bottom to the top of the pellet. One of these two then extinguished and the second became big-

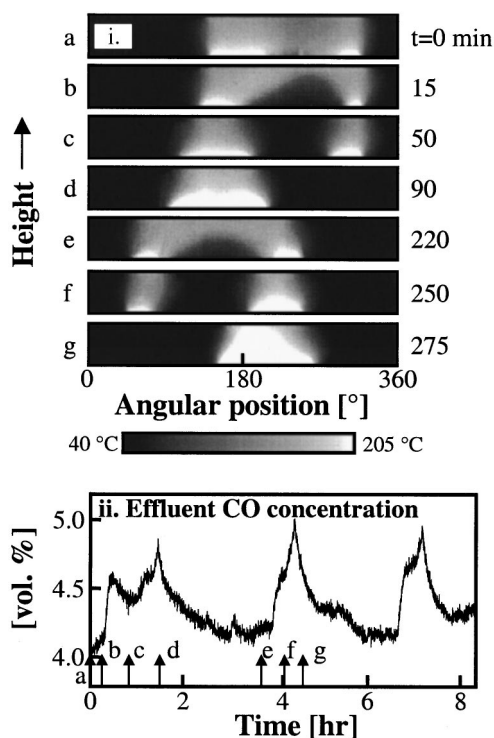


FIG. 9. Formation and extinction of hot zones on the side of the upside down turned pellet when the reactor is at 39 °C and the feed rate is 1600 cm<sup>3</sup>/min. (i) The instantaneous surface temperature on the sides at different times. (ii) The corresponding effluent CO concentration profile.

ger. At  $t=220$  min the hot region split into two. One of these extinguished between 250 and 275 min causing the other one to grow. The axial as well as the azimuthal location of the ignited regions changed from one period to the other. When the pellet was not turned upside down, a hot zone existed only at the top of the pellet under the same conditions (Fig. 5).

#### IV. DISCUSSION OF RESULTS

The temperature profiles observed on the catalytic hollow cylinder were much more intricate than those observed previously on a catalytic ring on which the same reaction was carried out.<sup>30,31</sup> Temperature gradients existed in both azimuthal and axial direction. No radial temperature gradients were observed on the top of the thin hollow cylinder in all the experiments. While the temperature patterns observed on the top of the hollow pellet were qualitatively similar to those observed on a thin ring,<sup>30,31</sup> the temperature patterns on the pellet side show that these patterns are more intricate than those on a thin ring, and that in many cases the temperatures on the top and bottom of the pellet were different.

Most theoretical and experimental studies of pattern formation are of diffusion-reaction systems. The patterns observed in our studies are affected by two additional factors; (1) global coupling and (2) the nonuniformity of the catalyst activity, the transport coefficients and the flow in the reactor. The global coupling is caused by the interaction between the overall reaction rate and the finite rate of the feed of reactants to the reactor.<sup>19,22,32</sup> A local increase (decrease) of the reaction rate at some location on the pellet decreases (increases) the reactant concentration in the reactor. This, in turn, decreases (increases) the reaction rate and temperature at all the other points on the surface. Thus, each point is affected by the reaction rate at all other points. The global coupling in this system stabilizes temperature fronts and patterns that would not have been stable otherwise, and counteracts any changes in the reactant concentration in the vessel. The reaction rate in the hot zone is significantly higher than that in the cold region. Thus, global coupling attempts to keep constant the total size of the hot zones. When one hot spot is extinguished, such as shown in Figs. 3, 4 and 9, the size of the remaining one increases. Similarly, the global coupling attempts to maintain a constant total reaction rate, counteracting any changes in the distance between two moving fronts, such as those in Figs. 5 and 7. The influence of the global coupling can be reduced by increasing the flow rate of the reactants to the reactor. Thus, the increase in the flow rate decreased the range of reactor temperatures for which a nonuniform state was obtained.

It is well known that it is extremely difficult to prepare supported heterogeneous catalytic pellets having uniform activity. This is further complicated by the reaction-induced nonuniform change of activity. All previous studies of spatiotemporal patterns during atmospheric reactions on heterogeneous catalysts were affected by this nonuniformity.<sup>11,14,30,31,33,34</sup> Theoretical studies of the impact of catalyst nonuniformity on observed patterns were reported among others by Liauw *et al.*,<sup>20</sup> Sheintuch,<sup>22</sup> Bär *et al.*,<sup>35</sup>

Bangia *et al.*,<sup>36</sup> Schütz *et al.*<sup>37</sup> and Hagberg *et al.*<sup>38</sup> The change in the temperature patterns when the catalyst is turned upside down is a clear manifestation of the nonuniformity of the catalytic activity. In most, but not all, cases, rotation of the pellet around the vertical axis did not change the azimuthal location of the pattern. This indicates that the flow and corresponding transport coefficients are azimuthally not uniform. In addition, the heat and mass transfer coefficients along the pellet side, bottom and top are not uniform and this enhances the formation of zones with different temperatures. The nonuniformities often constrain the movement of temperature fronts and hot zones and restrict them to certain regions on the catalyst. For example, the restricted movements of the temperature pulses in Figs. 4 and 5 are most probably caused by the inherent nonuniformities. A similar impact of the nonuniformities on the temperature patterns on a thin catalytic ring was reported by Annamalai *et al.*,<sup>30</sup> Liauw *et al.*,<sup>31</sup> and Somani *et al.*<sup>39</sup>

Backward motion of a pulse is usually prevented by the inhibitor present in the refractory region of the pulse. However, pulse splitting and wave reversal (backfiring) may be induced by local transitions in the state of a system from an excitable to a bistable one. It was observed previously among others by Sevcikova *et al.*<sup>40</sup> in a one-dimensional Belousov–Zhabotinskii reaction system under the influence of an electric field and by Bär *et al.*<sup>41</sup> during low pressure CO oxidation on Pt(110). The latter behavior was attributed to the existence of local inhomogeneities. It should, however, be noted that Bär *et al.*<sup>42</sup> and Mimura and Nagayama<sup>43</sup> observed backfiring in simulations of spatially homogeneous media. Our experiments revealed backfiring on both the pellet top (Figs. 3, 4, and 6) and side (Fig. 9). In the periodic pulse splitting shown in Fig. 4, each period consisted of two pulse splitting followed by extinction of one at two different angular locations. In other experiments (not shown here) the period consisted of a repeated pulse splitting at the same location. The pulse splitting may have been caused by a local nonuniformity which led to a shift from excitable to bistable dynamics as in the experiments by Bär *et al.*<sup>41</sup> It may have also been caused by the interaction between the local reaction dynamics on the pellet and the global coupling. The extinction of the pulses at the two angular locations is most probably due to the nonuniform catalyst activity. The global coupling causes the rapid growth (expansion) of one hot zone as the other is extinguished. Decreasing the reactor temperature decreased the overall reaction rate and increased the CO concentration in the reactor. This, in turn, decreased the size of the hot zone, but increased its maximal temperature and destabilized the temperature fronts (Fig. 7). An extensive analysis of front bifurcations was presented by Hagberg and Meron.<sup>44</sup> In reaction-diffusion systems the destabilization of stationary fronts is associated with an increase of  $R$ , the ratio of the time constant of the inhibitor to that of the activator. In our system the temperature is the activator and its time constant  $\tau_\theta$  is equal to  $\rho c_p / ha_v$ , where  $\rho$  and  $c_p$  are the pellet density and the heat capacity,  $h$  the heat transfer coefficient and  $a_v$  the heat transfer area per unit volume of catalyst. The dynamics of the system may be determined by more than two dynamic variables. In our system inhibition may be

caused by the surface activity and/or the reactant concentration. The time constant  $\tau_r$  of the reaction is  $1/k(T_r)$ , where  $k(T_r)$  is the reaction rate constant. Thus,  $R$ , the ratio of these two time constants equals  $ha_v / (k(T_r)\rho c_p)$ . This ratio increases as the temperature decreases, (due to the decrease in  $k(T_r)$ ) decreasing the stability of the temperature fronts. In the absence of global coupling the destabilization usually leads to a pitchfork bifurcation and a breathing motion of the pulse. A smooth transition of a standing pulse to traveling pulse is also possible, in the absence of global coupling, as demonstrated by Mimura and Nagayama.<sup>43</sup> Krischer and Mikhailov<sup>45</sup> showed that in the presence of global coupling an increase of  $R$  might cause a transition to a moving pulse. The strength of the coupling determines whether the transition is subcritical or supercritical. The meandering motions at low temperatures, shown in Figs. 5 and 7 (50 °C), are caused by such a destabilization. The nonuniformity of the catalyst which restricts the pulse motion leads to the back and forth motion. The temporal CO effluent concentrations obtained at low reactor temperatures (see Figs. 4 and 6) are rather irregular. Unfortunately, the very low frequency of these motions makes their proper analysis unpractical.

The experiments with the hollow cylinder strongly suggest that very rich and complex temperature patterns may evolve on three-dimensional catalysts which are widely used in the industry. In particular, it is of importance to understand and be able to predict their impact on the catalytic reaction rate and selectivity. Proper description and understanding of the patterns is also crucial for proper control measures.<sup>46</sup> The presence of global coupling and catalyst nonuniformity increases significantly the possible types of patterns. Many other important systems, such as muscles and other tissues, are intrinsically nonuniform. The impact of nonuniformity of the heart muscle on electrical potential motion was described by Winfree<sup>47</sup> and the March 1998 focus issue of this journal. The spatiotemporal patterns observed on electrochemical systems are also affected by both nonuniformity and global coupling.<sup>48–50</sup> A strong influence of reaction-induced surface restructuring was observed even during ultrahigh vacuum reactions on a cylindrical Pt single crystal.<sup>51,52</sup> Our experiments and those on heart fibrillations and electrochemical systems point out the need to gain a better understanding of pattern evolution in two and three dimensional bodies, and in particular those which are affected by local nonuniformities and global coupling.

## ACKNOWLEDGMENTS

This work was supported by grants from the National Science Foundation, the Welch Foundation, NATO CRG program and the BMBF (Liebig grant). We are most thankful to A. Mikhailov for many discussions and stimulating suggestions.

<sup>1</sup>M. C. Cross and P. C. Hohenberg, *Rev. Mod. Phys.* **65**, 851 (1993).

<sup>2</sup>M. Eiswirth and G. Ertl, in *Chemical Waves and Patterns*, edited by R. Kapral and K. Showalter (Kluwer, Dordrecht, 1994).

<sup>3</sup>G. Ertl and R. Imbihl, *Chem. Rev.* **95**, 697 (1995).

<sup>4</sup>H. Busch, *Ann. Phys. (Leipzig)* **64**, 401 (1921).

<sup>5</sup>V. Barelko, I. I. Kurochka, A. G. Merzhanov, and K. G. Shkadinskii, *Chem. Eng. Sci.* **33**, 805 (1978).

- <sup>6</sup>L. L. Lobban, G. Philippou, and D. Luss, *J. Phys. Chem.* **93**, 733 (1989).
- <sup>7</sup>L. L. Lobban and D. Luss, *J. Phys. Chem.* **93**, 6530 (1989).
- <sup>8</sup>M. Sheintuch and J. Schmidt, *J. Phys. Chem.* **92**, 3404 (1988).
- <sup>9</sup>G. A. Cordonier and L. D. Schmidt, *Chem. Eng. Sci.* **44**, 1983 (1989).
- <sup>10</sup>G. A. Cordonier, F. Schüth, and L. D. Schmidt, *J. Chem. Phys.* **91**, 5374 (1989).
- <sup>11</sup>G. Philippou, F. Schultz, and D. Luss, *J. Phys. Chem.* **95**, 3224 (1991).
- <sup>12</sup>G. Philippou and D. Luss, *Chem. Eng. Sci.* **48**, 2313 (1993).
- <sup>13</sup>J. R. Brown, G. A. D'Netto, and R. A. Schmitz, in *Temporal Order*, edited by L. Rensing and N. I. Jaeger (Springer, Berlin, 1985), p. 86.
- <sup>14</sup>P. C. Pawlicki and R. A. Schmitz, *Chem. Eng. Prog.* **83**, 40 (1987).
- <sup>15</sup>M. Somani, M. A. Liauw, and D. Luss, *Chem. Eng. Sci.* **51**, 4259 (1996).
- <sup>16</sup>S. L. Lane and D. Luss, *Phys. Rev. Lett.* **70**, 830 (1993).
- <sup>17</sup>M. D. Graham, S. L. Lane, and D. Luss, *J. Phys. Chem.* **97**, 7564 (1993).
- <sup>18</sup>S. Y. Yamamoto, C. M. Surko, M. B. Maple, and R. K. Pina, *J. Chem. Phys.* **102**, 8614 (1995).
- <sup>19</sup>U. Middy, D. Luss, and M. Sheintuch, *J. Chem. Phys.* **100**, 3568 (1994).
- <sup>20</sup>M. A. Liauw, J. Ning, and D. Luss, *J. Chem. Phys.* **104**, 5657 (1996).
- <sup>21</sup>S. Shvartsman, A. K. Bangia, M. Bär, and I. G. Kevrekidis, in *Disordered Media, IMA Volume on Mathematics and its Applications*, edited by K. Golden, G. Grimmett, G. Milton, and P. Sen (Springer, Berlin, 1997).
- <sup>22</sup>M. Sheintuch, *J. Phys. Chem.* **100**, 15137 (1996).
- <sup>23</sup>J. C. Kellow and E. E. Wolf, *Chem. Eng. Sci.* **45**, 2597 (1990).
- <sup>24</sup>C.-C. Chen, E. E. Wolf, and H.-C. Chang, *J. Phys. Chem.* **97**, 1055 (1993).
- <sup>25</sup>F. Qin and E. E. Wolf, *Chem. Eng. Sci.* **50**, 117 (1995).
- <sup>26</sup>S. L. Lane, M. D. Graham, and D. Luss, *AIChE. J.* **39**, 1497 (1993).
- <sup>27</sup>J. L. Hudson and T. T. Tsotsis, *Chem. Eng. Sci.* **49**, 1493 (1994).
- <sup>28</sup>M. T. M. Koper, *J. Chem. Soc., Faraday Trans.* **94**, 1369 (1998).
- <sup>29</sup>K. Krischer, in *Modern Aspects of Electrochemistry*, edited by J. O'M. Bockris, B. E. Conway, and R. E. White (Plenum, New York, 1998).
- <sup>30</sup>J. Annamalai, C. Ballandis, M. Somani, M. A. Liauw, and D. Luss, *J. Chem. Phys.* **107**, 1896 (1997).
- <sup>31</sup>M. A. Liauw, M. Somani, J. Annamalai, and D. Luss, *AIChE. J.* **43**, 1519 (1997).
- <sup>32</sup>M. Sheintuch and S. Shvartsman, *AIChE. J.* **42**, 1041 (1996).
- <sup>33</sup>J. C. Kellow and E. E. Wolf, *AIChE. J.* **37**, 1844 (1991).
- <sup>34</sup>G. Philippou and D. Luss, *J. Phys. Chem.* **96**, 6651 (1992).
- <sup>35</sup>M. Bär, I. G. Kevrekidis, H.-H. Rotermund, and G. Ertl, *Phys. Rev. E* **52**, 5739 (1995).
- <sup>36</sup>A. K. Bangia, M. Bär, I. G. Kevrekidis, M. D. Graham, H.-H. Rotermund, and G. Ertl, *Chem. Eng. Sci.* **51**, 1757 (1996).
- <sup>37</sup>P. Schütz, M. Bode, and H.-G. Purwins, *Physica D* **82**, 382 (1995).
- <sup>38</sup>A. Hagberg, E. Meron, I. Rubinstein, and B. Zaltzman, *Phys. Rev. Lett.* **76**, 427 (1996).
- <sup>39</sup>M. Somani, M. A. Liauw, and D. Luss, *Chem. Eng. Sci.* **52**, 2331 (1997).
- <sup>40</sup>H. Sevcikova, M. Marek, and S. C. Müller, *Science* **257**, 951 (1992).
- <sup>41</sup>M. Bär, M. Eiswirth, H.-H. Rotermund, and G. Ertl, *Phys. Rev. Lett.* **69**, 945 (1992).
- <sup>42</sup>M. Bär, M. Hildebrand, M. Eiswirth, M. Falcke, H. Engel, and M. Neufeld, *Chaos* **4**, 499 (1994).
- <sup>43</sup>M. Mimura and M. Nagayama, *Chaos* **7**, 817 (1997).
- <sup>44</sup>A. Hagberg and E. Meron, *Nonlinearity* **7**, 805 (1994).
- <sup>45</sup>K. Krischer and A. Mikhailov, *Phys. Rev. Lett.* **73**, 3165 (1994).
- <sup>46</sup>S. Y. Shvartsman and I. G. Kevrekidis, *AIChE. J.* **44**, 1579 (1998).
- <sup>47</sup>A. T. Winfree, *Int. J. Bifurcation Chaos Appl. Sci. Eng.* **7**, 487 (1997).
- <sup>48</sup>O. Lev, M. Sheintuch, H. Yarnitzky, and L. M. Pismen, *Chem. Eng. Sci.* **45**, 839 (1990).
- <sup>49</sup>R. D. Otterstedt, P. J. Plath, N. I. Jaeger, and J. L. Hudson, *J. Chem. Soc., Faraday Trans.* **92**, 2933 (1996).
- <sup>50</sup>N. Mazouz, G. Flätgen, K. Krischer, and I. G. Kevrekidis, *J. Electrochem. Soc.* **147**, 2404 (1998).
- <sup>51</sup>M. Sander, G. Veser, and R. Imbihl, *J. Vac. Sci. Technol. A* **10**, 2495 (1992).
- <sup>52</sup>G. Veser and R. Imbihl, *Surf. Sci.* **269/270**, 465 (1992).